Angular dependence of light transmittance in polymer dispersed liquid crystals

F. Bloisi, C. Ruocchio, P. Terrecuso, and L. Vicari
Istituto Nazionale per la Fisica della Materia, Dipartimento di Scienze Fisiche, Università di Napoli ''Federico II,'' Piazzale Vincenzo Tecchio 80, I 80125 Napoli, Italy

(Received 12 February 1996; revised manuscript received 24 July 1996)

Polymer dispersed liquid crystals (PDLC's) are composite materials made of a dispersion of liquid-crystal droplets in a polymeric matrix. The droplets appear as highly optically anisotropic spheres with random orientation. Light impinging on a film of this material is almost entirely scattered unless the application of an electric field aligns the liquid-crystal molecules inside the droplets so that all droplets behave as uniaxial media aligned to the applied field. If the polymer refractive index is equal to the ordinary refractive index of the liquid crystal the sample becomes transparent for normally impinging light. Unlike common glass, the angular dependence of light transmittance is not given by Fresnel relations but is a fairly intricate function of the liquid-crystal distribution inside the droplets. In the framework of the general theory of PDLC's by Palffy-Muhoray and co-workers [Mol. Cryst. Liq. Cryst. **243**, 11 (1994); **179**, 445 (1990)], using the anomalous diffraction approach scattering by Zumer [Phys. Rev. A **37**, 4006 (1988)], we introduce a mathematical model of PDLC transparency versus applied voltage and the incidence angle. Experimental results are presented. The experimental results correspond well to the theoretical results. [S1063-651X(96)11911-5]

PACS number(s): 61.30.Gd, 42.25.Fx, 61.30.Cz

I. INTRODUCTION

Polymer dispersed liquid crystals (PDLC's) are nonhomogeneous materials consisting of liquid crystal droplets randomly dispersed in a polymeric matrix [1–6]. Commonly used liquid crystals are in the nematic phase at room temperature and therefore droplets appear as highly optically anisotropic spheres having random orientation so that light impinging on a PDLC film is almost entirely scattered. Application of an electric field aligns the liquid-crystal molecules inside the droplets so that all droplets behave as uniaxial media aligned with the applied field; if the polymer refractive index is equal to the ordinary refractive index of the liquid crystal the scattering for normally impinging light is reduced to zero and the sample becomes transparent [7]. Thus a PDLC film behaves as an electrically controlled light shutter where light scattering is the main switching mechanism, while absorption is negligible. This behavior is useful in many applications such as switchable windows or direct view displays. The properties of PDLC films are also interesting in understanding the distribution of highly anisotropic molecules confined in small volumes. Many authors [8–16], have dealt with the fundamental problem of liquid-crystal molecular director distribution and its consequences on the light scattering.

Since the PDLC film light transmission ratio is due to both reflection at film surfaces and scattering in the bulk, the angular dependence of light transmittance is not simply given by Fresnel relations, but is a quite intricate function of the liquid-crystal distribution inside the droplets. In previous papers [14,15] we introduced a mathematical model of the molecular behavior of the sample in order to deal with the phase shift of a light ray through it. Then we applied it to sample transmittance during the electro-optical transition for normal incidence of light. A recent Letter [17] has been devoted to the angular dependence of light transmittance through these electro-optic films for the particular case of device operated in the ''above-threshold'' condition, i.e., just above the transition to its transparent state. In this paper we will extend our investigation on the angular dependence of light transmission ratio to the whole transition from the translucent to the transparent state versus the applied voltage. The phenomenon is studied from both a theoretical and an experimental point of view. Our theory is developed in the framework of Palffy-Muhoray and co-workers [18,19] approach to the optical description of liquid crystals in PDLC's, while for the scattering by the droplets we use the anomalous diffraction approach (ADA) scattering theory [20]. On this basis a mathematical model of the PDLC behavior is constructed and operated on a personal computer. An experimental setup has been realized in order to verify theoretical predictions by the execution of measurements. The experimental results correspond well to the theoretical results. We conclude by using the model to study the sample angular transmittance versus some optical and geometrical parameters.

II. THEORY

We consider a PDLC film bound between two conducting glass plates with an applied voltage generating a low-frequency (1 kHz) electric field **E**. A complete description of the scattered intensity distribution is difficult, but if we are only interested in the transmitted intensity, assuming that multiple scattering can be neglected, we can simply write

$$I_t = I_0 T_F \exp(-N_v \sigma_s d_0 / \cos\gamma_p), \tag{1}$$

where I_0 is the incident light intensity, N_v is the number of droplets per unit volume, d_0 is the PDLC film thickness, $\gamma_p = \arcsin(\sin\gamma_i / n_p)$ gives the beam propagation direction inside the polymer, γ_i is the incidence angle, n_p is the polymer refractive index, $T_F = T_{ag} T_{gp} T_{pg} T_{ga}$ are the Fresnel transmission coefficients [21] at air-glass, glass-polymer,

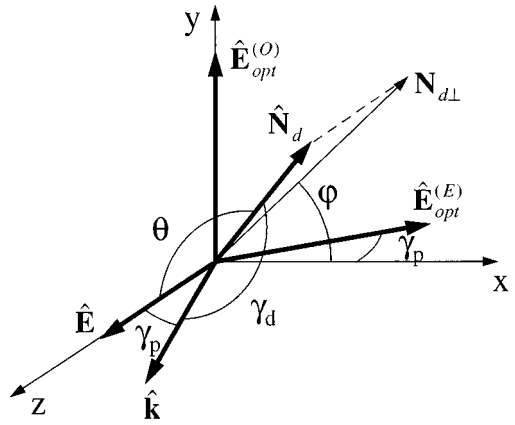

FIG. 1. Reference frame. Axes are chosen so that the xy plane is the surface of the sample and the xz plane is the incidence plane. The external field $\mathbf{E}$ is in the direction of the z axis and the wave vector $\mathbf{k}$ is in the xz plane. $\hat{\mathbf{N}}_d$ is the director of a generic droplet, while $\mathbf{N}_{d\perp}$ is the projection of $\hat{\mathbf{N}}_d$ on the xy plane. γ_p and γ_d are the beam incidence angles with respect to the sample and the droplet, respectively. The optical electric field $\mathbf{E}_{\rm opt}$ is either in the direction of the y axis ($\mathbf{E}^{(O)}_{\rm opt}$ ordinary beam) or in the xz plane ($\mathbf{E}^{(E)}_{\rm opt}$ extraordinary beam).

polymer-glass, and glass-air interfaces, respectively, and $\sigma_s=\langle\sigma_d\rangle_{\rm sample}$ (i.e., the average of the droplet scattering cross section σ_d over the whole sample) is the sample scattering cross section.

Each droplet behaves as a uniaxial transparent medium with a different symmetry axis, but the direction of the applied electric field defines a preferred axis so that the whole sample behaves as a uniaxial medium. We must therefore distinguish between ordinary (polarization plane orthogonal to the incidence plane) and extraordinary (polarization plane in the incidence plane) impinging beams. Since usually the polymer refractive index n_p is almost equal to the glass one n_g, we neglect the terms $T_{gp}T_{pg}$ so that for an extraordinary and an ordinary beam we have, respectively,

$$T_F^{(E)}=\left[\frac{4\,\sin\gamma_g\sin\gamma_i\cos\gamma_g\cos\gamma_i}{\sin^2(\gamma_g+\gamma_i)\cos^2(\gamma_g-\gamma_i)}\right]^2, \tag{2a}$$

$$T_F^{(O)}=\left[\frac{4\,\sin\gamma_g\sin\gamma_i\cos\gamma_g\cos\gamma_i}{\sin^2(\gamma_g+\gamma_i)}\right]^2, \tag{2b}$$

where $\gamma_g=\arcsin(\sin\gamma_i/n_g)$ gives the beam propagation direction inside the glass.

In order to compute the sample scattering cross section σ_s we have to average the droplet scattering cross section σ_d over all droplet orientations

$$\sigma_s=\int_0^{2\pi}d\varphi\int_0^{\pi}\sigma_d(\vartheta,\varphi)p_d(\vartheta,\varphi)\sin\vartheta\,d\vartheta, \tag{3}$$

where $p_d(\vartheta,\varphi)d\Omega$ is the probability of the droplet director $\hat{\mathbf{N}}_d$ of being in the solid angle $d\Omega=\sin\vartheta d\vartheta d\varphi$. Without loss of generality we have assumed (see Fig. 1) that the sample surface is orthogonal to the z direction (i.e., the electric field $\mathbf{E}$ is in the z direction) and the incidence plane is the xz plane (i.e., the wave vector $\mathbf{k}$ has zero y component). For a single spherical droplet of radius R, the scattering cross section $\sigma_d(\vartheta,\varphi)$ (ϑ and φ giving the orientation of droplet director), according to the ADA theory, is [20]

$$\sigma_d=\frac{1}{2}\sigma_G(2kR)^2\left[\left(\frac{n^*_{de}}{n_p}-1\right)^2\cos^2\alpha_d+\left(\frac{n^*_{do}}{n_p}-1\right)^2\sin^2\alpha_d\right], \tag{4}$$

where $\sigma_G=\pi R^2$ is the droplet geometrical cross section, $k=2\pi/\lambda$ is the impinging beam wave number, α_d is the polarization angle with respect to the droplet, i.e., the angle between the polarization plane (containing the polarization vector $\hat{\mathbf{E}}_{\rm opt}$ and $\hat{\mathbf{k}}$) and the droplet incidence plane (containing $\hat{\mathbf{N}}_d$ and $\hat{\mathbf{k}}$), and n^*_{do} and n^*_{de} are the effective (ordinary and extraordinary) refractive indices of the scattering sphere, for light impinging with direction $\hat{\mathbf{k}}$. Obviously $n^*_{do}=n_{do}$ does not depend on the incidence angle, while n^*_{de} is given by

$$n^*_{de}=\frac{n_{do}n_{de}}{\sqrt{n^2_{do}\sin^2\gamma_d+n^2_{de}\cos^2\gamma_d}}, \tag{5}$$

where n_{do} and n_{de} are the ordinary and extraordinary droplet refractive indices and (see Fig. 1)

$$\gamma_d=\arccos(\sin\vartheta\cos\varphi\sin\gamma_p+\cos\vartheta\cos\gamma_p) \tag{6}$$

is the incidence angle with respect to the droplet, i.e., the angle between the beam wave vector $\hat{\mathbf{k}}\equiv(\sin\gamma_p,0,\cos\gamma_p)$ and the droplet director $\hat{\mathbf{N}}_d\equiv(\sin\vartheta\cos\varphi,\sin\vartheta\sin\varphi,\cos\vartheta)$. The droplet refractive indices are functions of the orientation of the liquid-crystal molecules inside the droplet, i.e. of the droplet order parameter S_d defined as $S_d=\langle P_2(\hat{\mathbf{N}}_d\cdot\hat{\mathbf{n}})\rangle_{\rm droplet}$ where $\hat{\mathbf{n}}$ is the nematic director, $P_2(x)$ is the second-order Legendre polynomial, and the average is taken over each droplet. The behavior of the liquid-crystal molecules inside droplets depends on many parameters (such as the liquid-crystal elastic constants, the droplet radius, the type of alignment at the droplet surface). However, it has been calculated [22] that the bipolar configuration is energetically preferred in the case of tangential anchoring: molecules are strongly aligned with the droplet director $\hat{\mathbf{N}}_d$, with two disclinations at the ''poles'' of the droplet. This configuration is commonly used since it gives high contrast and low driving voltages. In a previous paper [14] we have shown that, for such configuration, the droplet refractive indices can be computed with good approximation assuming that all nematic directors are at the same angle with respect to the droplet director. This assumption leads to the expressions

$$n_{do}=\frac{2}{\pi}n_oF\left(\frac{\pi}{2},\frac{1}{n_e}\sqrt{\frac{2}{3}(n_e^2-n_o^2)(1-S_d)}\right), \tag{7a}$$

$$n_{de}=\frac{n_on_e}{\sqrt{\frac{2}{3}(n_o^2-n_e^2)S_d+\frac{1}{3}(n_o^2+2n_e^2)}}, \tag{7b}$$

where $F(\theta,m)$ is the complete elliptic integral of the first kind and n_o and n_e are the liquid crystal refractive indices. A value $S_d=1$ for the droplet order parameter means that the

local nematic director is aligned with the droplet director everywhere, so that, as expected, $n_{de}|_{S_d=1}=n_e$ and $n_{do}|_{S_d=1}=n_o$. Usually the optical anisotropy of the liquid crystal is small, so that we can assume $(n_{de}-n_{do})/n_{do}\ll 1$; thus expanding n_{de}^* in terms of $(n_{de}-n_{do})$ we can approximate Eq. (5) with

$$n_{de}^* \simeq n_{do}+(n_{de}-n_{do})\sin^2\gamma_d . \tag{8}$$

Therefore Eq. (4) becomes

$$\sigma_d=\frac{1}{2}\sigma_G(2kR)^2(s_e^2\cos^2\alpha_d+s_o^2\sin^2\alpha_d), \tag{9}$$

where

$$s_e=\frac{n_{de}-(n_{de}-n_{do})\cos^2\gamma_d}{n_p}-1, \tag{10a}$$

$$s_o=\frac{n_{do}}{n_p}-1. \tag{10b}$$

This allows the sample scattering cross section (3) to be written as

$$\sigma_s=\frac{1}{2}\sigma_G(2kR)^2\int_0^{2\pi}d\varphi \times\int_0^{\pi}(s_e^2\cos^2\alpha_d+s_o^2\sin^2\alpha_d)p_d(\vartheta,\varphi)\sin\vartheta d\vartheta. \tag{11}$$

Nevertheless, it is not possible to carry out the integrations since we still do not know the probability distribution $p_d(\vartheta,\varphi)$. This distribution is determined by the external field **E** starting from the original uniform distribution

$$p_d(\vartheta(\tilde{\vartheta},\tilde{\varphi}),\varphi(\tilde{\vartheta},\tilde{\varphi}))d\tilde{\Omega}=\frac{d\tilde{\Omega}}{4\pi}, \tag{12}$$

where $\tilde{\vartheta}$ and $\tilde{\varphi}$ are the values of ϑ and φ in the absence of the external field. Therefore we need to express the droplet scattering cross section $\sigma_d(\vartheta,\varphi)$ as a function of the droplet director orientation $(\tilde{\vartheta},\tilde{\varphi})$ before the field is applied. Due to the choice of the reference frame, only ϑ is affected by the external field: therefore $\varphi(\tilde{\vartheta},\tilde{\varphi})=\tilde{\varphi}$, while $\vartheta(\tilde{\vartheta},\tilde{\varphi})=\vartheta(\tilde{\vartheta})$ can be obtained minimizing the free energy for a droplet in an external electric field. Following Kelly and Palffy-Muhoray [18] the free energy per volume can be written as an elastic term plus a term due to the external electric field.

The elastic term is

$$\mathcal{F}_{\rm el}=-\frac{1}{3}K_dP_2(\hat{\mathbf{N}}_d\cdot\hat{\tilde{\mathbf{N}}}_d), \tag{13}$$

where K_d is an elastic constant per unit volume taking into account the torque that, after the field is switched off, produces relaxation of the droplet director $\hat{\mathbf{N}}_d$ to its original orientation $\hat{\tilde{\mathbf{N}}}_d$, while the field related term is

$$\mathcal{F}_E=-\frac{1}{3}g(S_s)SS_d(\varepsilon_\parallel-\varepsilon_\perp)\mathbf{E}^2P_2(\hat{\mathbf{N}}_d\cdot\hat{\mathbf{E}}) \tag{14}$$

where **E** is the applied electric field,

$$g(S_s)=\frac{3\,\varepsilon_p v_{\rm LC}}{\varepsilon_{\rm LC}+2\varepsilon_p-v_{\rm LC}(\varepsilon_{\rm LC}-\varepsilon_p)}, \tag{15}$$

$$\varepsilon_{\rm LC}=\varepsilon_\perp+\frac{1}{3}(1+2SS_dS_s)(\varepsilon_\parallel-\varepsilon_\perp), \tag{16}$$

S and S_s, defined as

$$S=\langle P_2(\hat{\mathbf{n}}\cdot\hat{\boldsymbol{l}})\rangle, \tag{17a}$$

$$S_s=\langle P_2(\hat{\mathbf{E}}\cdot\hat{\mathbf{N}}_d)\rangle_{\rm sample} \tag{17b}$$

are the usual molecular order parameter and the sample order parameter, $\hat{\boldsymbol{l}}$ is the molecular axis, $\hat{\mathbf{n}}$ is the nematic director, $v_{\rm LC}$ is the volume fraction of liquid crystal in the sample, ε_p is the polymer dielectric permittivity, $\varepsilon_\parallel$ and $\varepsilon_\perp$ are the liquid-crystal dielectric permittivities.

The droplet director $\hat{\mathbf{N}}_d$ is obtained by minimization of the total free energy $\mathcal{F}=\mathcal{F}_{\rm el}+\mathcal{F}_E$, which leads to [18]

$$P_2(\hat{\mathbf{N}}_d\cdot\hat{\mathbf{E}})=\frac{1}{4}+\frac{3}{4}\frac{e_a^2-1+2(\hat{\tilde{\mathbf{N}}}_d\cdot\hat{\mathbf{E}})^2}{\sqrt{(e_a^2-1)^2+4e_a^2(\hat{\tilde{\mathbf{N}}}_d\cdot\hat{\mathbf{E}})^2}} \tag{18}$$

or, since $\hat{\mathbf{N}}_d\cdot\hat{\mathbf{E}}=\cos\vartheta$ and $\hat{\tilde{\mathbf{N}}}_d\cdot\hat{\mathbf{E}}=\cos\tilde{\vartheta}$,

$$\vartheta(\tilde{\vartheta},S_s)=\arccos\sqrt{\frac{1}{2}[1+a(\tilde{\vartheta},S_s)]}, \tag{19}$$

where we have defined

$$a(\tilde{\vartheta},S_s)=\frac{e_a^2-1+2(\hat{\tilde{\mathbf{N}}}_d\cdot\hat{\mathbf{E}})^2}{\sqrt{(e_a^2-1)^2+4e_a^2(\hat{\tilde{\mathbf{N}}}_d\cdot\hat{\mathbf{E}})^2}} =\frac{e_a^2-1+2\cos^2\tilde{\vartheta}}{\sqrt{(e_a^2-1)^2+4e_a^2\cos^2\tilde{\vartheta}}} \tag{20}$$

and we have used the reduced electric field

$$e_a(S_s)=E\sqrt{\frac{3\,\varepsilon_p v_{lc}}{\varepsilon_{lc}+2\varepsilon_p-v_{\rm LC}(\varepsilon_{\rm LC}-\varepsilon_p)}\frac{\varepsilon_\parallel-\varepsilon_\perp}{K_d}}. \tag{21}$$

Therefore Eq. (11) becomes

$$\sigma_s=\int_0^{2\pi}d\tilde{\varphi}\int_0^{\pi}\sigma_d(\vartheta(\tilde{\vartheta},\tilde{\varphi}),\varphi(\tilde{\vartheta},\tilde{\varphi}))p_d(\vartheta(\tilde{\vartheta},\tilde{\varphi}),\varphi(\tilde{\vartheta},\tilde{\varphi})) \times\sin\tilde{\vartheta}d\tilde{\vartheta} =\frac{\sigma_G}{8\pi}(2kR)^2\int_0^{2\pi}d\varphi\int_0^{\pi}(\tilde{s}_e^2\cos^2\alpha_d+\tilde{s}_o^2\sin^2\alpha_d)\sin\tilde{\vartheta}d\tilde{\vartheta}, \tag{22}$$

with $\tilde{s}_o = s_o$ and

$$\tilde{s}_e = \frac{n_{de} - \frac{1}{2}(n_{de} - n_{do})[\sqrt{1 - a(\tilde{\vartheta}, S_s)}\cos\varphi\sin\gamma_p + \sqrt{1 + a(\tilde{\vartheta}, S_s)}\cos\gamma_p]^2}{n_p} - 1. \tag{23}$$

The sample order parameter S_s (17b), required to compute $\tilde{s}_e$, is the average over the whole sample of $P_2(\hat{\mathbf{N}}_d \cdot \hat{\mathbf{E}})$. Under the assumption that initial orientation of droplet directors $(\tilde{\hat{\mathbf{N}}}_d)$ is isotropic, using Eq. (18), we get

$$S_s = \langle P_2(\hat{\mathbf{E}} \cdot \hat{\mathbf{N}}_d)\rangle_{\text{sample}} = \langle P_2(\cos\vartheta)\rangle_{\text{sample}} = \int_0^{2\pi} d\tilde{\varphi} \int_0^{\pi} P_2(\cos\vartheta(\tilde{\vartheta}, S_s))\sin\tilde{\vartheta} d\tilde{\vartheta}, \tag{24}$$

which leads to

$$S_s = \frac{1}{4} + \frac{3}{16}\frac{e_a^2 + 1}{e_a^2} + \frac{3}{32}\frac{(3e_a^2 + 1)(e_a^2 + 1)}{e_a^3}\ln\left|\frac{e_a + 1}{e_a - 1}\right|. \tag{25}$$

Equation (25), together with Eqs. (21) and (16), constitutes a system of implicit relations allowing the computation of the sample order parameter S_s once molecular and droplet order parameters are known. In a previous paper [23] we have shown that, while the molecular order parameter S is unaffected by the applied electric field (it is just a function of the temperature), this is not the case for the droplet order parameter S_d: in the saturation region (i.e. field above the threshold value, $S_s \approx 1$, with droplet directors almost aligned with the field) the electric field aligns molecules with the droplet director and therefore increases the droplet order parameter S_d; on the contrary, below the transition region (i.e., field below the threshold value $S_s \ll 1$, with droplet directors randomly oriented) the electric field has a direction that differs from droplet director and therefore causes a decrease of droplet order parameter. We have shown [23] that a good expression for S_d is

$$S_d(E, S_s) = \sqrt{(2S_s + 1)/3}[1 - \exp(-E/E_{d1})] + S_{d0}\sqrt{1 - S_s}\exp(-E/E_{d2}), \tag{26}$$

where S_{d0} is the droplet order parameter in absence of field and E_{d1} and E_{d2} are two sample related parameters taking into account the dependence of the alignment of liquid-crystal molecules inside each droplet versus the external field and the sample order parameter. Now we have all the elements required to integrate Eq. (22) to obtain the sample scattering cross section and, by means of Eq. (1), the sample transmittance $\tau = I_t / I_0$.

III. EXPERIMENT

The experimental setup is shown in Fig. 2. The probe beam is a 2-mW HeNe laser ($\lambda = 632.8$ nm). Both the polarization plane and the incidence angle can be changed without changing the incidence point on the sample. A square wave electric signal is applied to the sample. The peak-to-peak intensity and the frequency of the signal can be controlled by means of a function generator and a voltage amplifier. The frequency is fixed at $\nu = 1$ kHz. The sample is contained in a thermostatic oven in order to keep its temperature constant to $T_0 = 25.5$°C. A photodiode (D_1, collection angle 0.4×10^{-3} sr) in a chopper–lock-in configuration is used to detect the signal. A second photodiode detector (D_2) is used to obtain a reference. The sample thickness is $d_0 = 20\mu$ m and the PDLC composition is the following: EPON 815 (Shell Chemical Company) 25.8%, MK 107 (Wilmington Chemical Corporation) 7.4%, CAPCURE 3-800 (Diamond Shamrock & Co.) 30.2%, BOSTIK B (Bostik) 3.4%, and E7 (BDH) 33.3%. The refractive indices of E7 are $n_o = 1.51$ and $n_e = 1.74$ and its nematic to isotropic phase transition temperature, measured in the PDLC configuration, is $T_{NI} = 54.5$°C. The polymer refractive index is $n_p = 1.54$ and

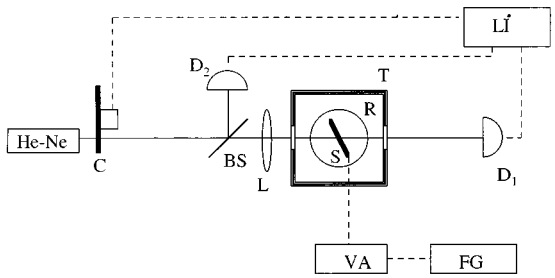

FIG. 2. Experimental setup. HeNe, 2-mW He-Ne laser mounted on a rotating support; C, chopper; BS, beam splitter; L, lens; D1,D2, photodiode detectors; T, thermostatic oven; R, rotation stage; S, sample; LI, lock-in amplifier; FG, function generator; VA, voltage amplifier.

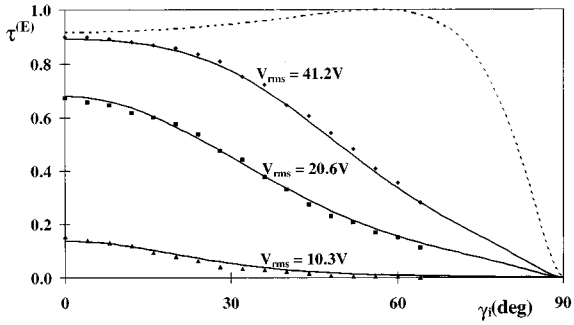

FIG. 3. Angular dependence of the transmittance for an extraordinary beam, for different values of the applied field ($V_{\text{rms}} = 10.3$, 20.6, and 41.2 V). Experimental values (dots) are compared with theoretical results (solid curves). Experimental errors are within dot size. The dashed line is the transmittance of the cell without PDLC.

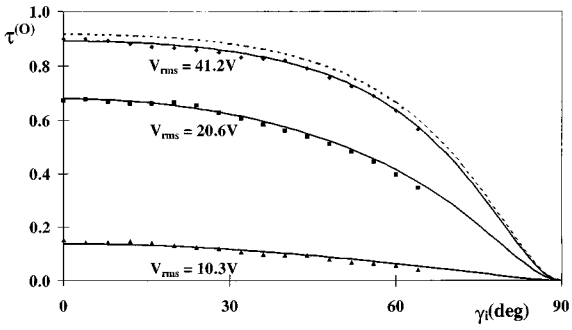

FIG. 4. Angular dependence of the transmittance for an ordinary beam, for different values of the applied field ($V_{\rm rms}=10.3$, 20.6, 41.2 V). Experimental values (dots) are compared with theoretical results (solid curves). Experimental errors are within dot size. The dashed line is the transmittance of the cell without PDLC.

the glass refractive index $n_g=1.52$.

In Fig. 3 we report the sample light transmittance versus the incidence angle for different values of the applied voltage for the polarization plane in the incidence plane (extraordinary beam). Experimental results are shown by dots and errors are within dot size.

To apply our model to an impinging extraordinary beam, we observe (see Fig. 1) that $\hat{\mathbf{E}}_{\rm opt}^{(E)}\equiv(\cos\gamma_p,0,\sin\gamma_p)$, so that the polarization angle with respect to the droplet α_d is given by

$$\alpha_d^{(E)}=\arcsin\frac{\cos 2\gamma_p\sin\vartheta\sin\varphi}{\sqrt{1-(\sin\vartheta\cos\varphi\sin\gamma_p+\cos\vartheta\cos\gamma_p)^2}}. \quad (27)$$

Substitution into Eq. (22) gives the droplet scattering cross section for an extraordinary beam.

Solid curves in Fig. 3 are computed by the described theory, while the dashed curve is the theoretical transmittance of the glasses, without PDLC's, simply given by Fresnel transmission coefficients (2). The values of the parameters used for description of our sample are droplet radius $R=1\ \mu$m, droplets per unit volume $N_v=0.143\times10^{18}\ \mathrm{m}^{-3}$, and in Eqs. (21) and (26) $K_d=5.97\ \mathrm{Nm}^{-2}$, $S_{d0}=0.816$, $E_{d1}=3.33\times10^6\ \mathrm{Vm}^{-1}$, and $E_{d2}=1.00\times10^6\ \mathrm{Vm}^{-1}$. The liquid-crystal order parameter,

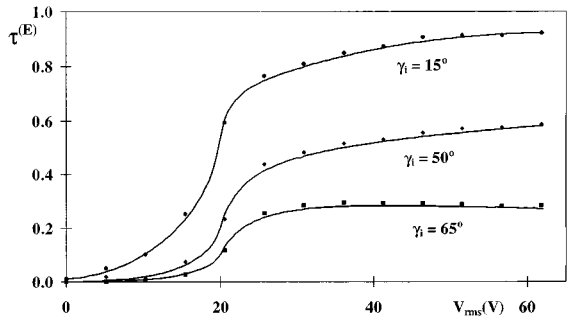

FIG. 5. Voltage dependence of the transmittance for an extraordinary beam, for different values of the incidence angle ($\gamma_i=15°$, 50°, and 65°). Experimental values (dots) are compared with theoretical results (solid curves). Experimental errors are within dot size.

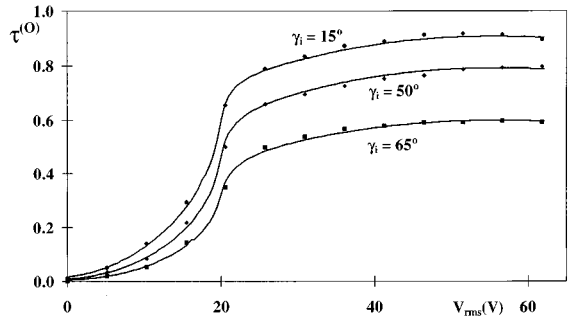

FIG. 6. Voltage dependence of the transmittance for an ordinary beam, for different values of the incidence angle ($\gamma_i=15°$, 50°, and 65°). Experimental values (dots) are compared with theoretical results (solid curves). Experimental errors are within dot size.

assumed to be a universal function of the temperature [10], is $S_{|T=25.5°\mathrm{C}}=0.611$. We have no direct measure of droplet radius in this sample; also because it is destructive, scanning electron microscopy performed on samples made with the same recipe confirmed the value of about $1\,\mu$m.

Figure 4 shows the same quantities for a beam with its polarization plane orthogonal to the incidence plane (ordinary beam). Experimental data are compared to theoretical results obtained with the same parameters as before, but with polarization angle $\alpha_d=\alpha_d^{(O)}=\pi/2-\alpha_d^{(E)}$ Again the dashed curve is the transmittance of the glasses alone.

Figures 5 and 6 show the dependence of the transmittance of the sample versus the applied voltage for an extraordinary and an ordinary beam, respectively. Experimental data (dots) obtained in an independent set of measurements are compared to results obtained by our model (solid curves) with the same values of the parameters. As can be seen, our mathematical model gives an accurate description of the experimental results for both the ordinary and the extraordinary components of an impinging beam.

IV. DISCUSSION AND CONCLUSION

The model we have described can be used to examine the transmittance of a PDLC in many situations and can be useful for designing PDLC devices. For the sake of simplicity and in order to perform a comparison with experimental data in previous figures we have only shown a few numerical results. The computer program based on our model does not

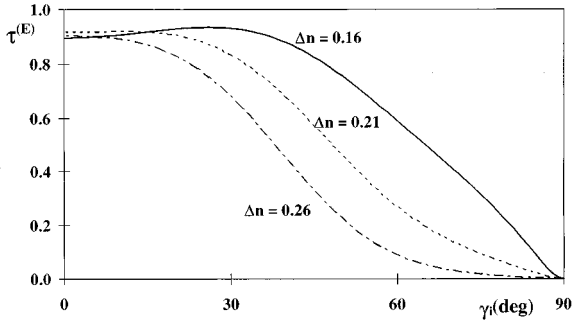

FIG. 7. Transmittance for an extraordinary beam vs the incidence angle for different values of the optical anisotropy of the liquid crystal $\Delta n=n_e-n_o$.

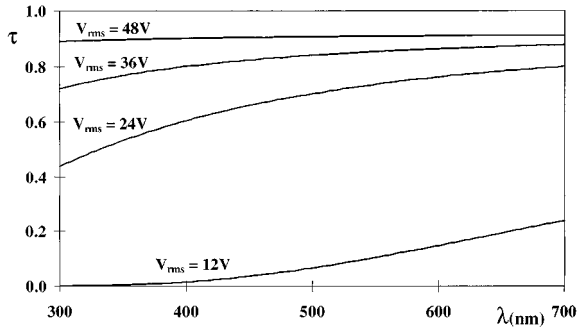

FIG. 8. Transmittance vs wavelength for different values of the applied voltage, at normal incidence ($\gamma_i = 0$).

require much computation time even on a personal computer, allowing easy examination of a large number of configurations.

The translucent to transparent state transition (Figs. 5 and 6) in our sample occurs at an applied voltage $V_{\mathrm{rms}}^{(\mathrm{thr})} \approx 21\ V$. For applied voltage above this threshold value (due to a sudden increase of the sample order parameter) the transmittance increases slightly, due to a further slight increase of the droplet order parameter. We observe (Figs. 3 and 4, $V_{\mathrm{rms}} = 41.2$ V) that for high enough applied voltage (saturation condition) and for normal incidence the transmittance of the PDLC sample is practically equal to the transmittance of the glass plates, while for high incidence angle the PDLC film practically affects only the extraordinary beam. This gives rise to a polarization effect on the light impinging at large incidence angles.

The most important optical parameter of the liquid crystal is the optical anisotropy $\Delta n = n_e - n_o$. Using our model to study the angular dependence of the transmittance on liquid crystal's optical anisotropy (Fig. 7), it can be seen that a larger liquid-crystal anisotropy makes the PDLC transmittance more angularly selective: the sample is transparent only for small incidence angles, while it is translucent for higher values of γ_i.

As a further application of the model we examine the effect of light scattering on the spectral composition of the transmitted light. Here we disregard light absorption by the sample. Even if we do not have measurements performed on these samples, experimental measures carried out on PDLC films having the same composition have shown that light absorption is negligible in the $350-800$ nm wavelength range. Figure 8 shows the sample transmittance for normal incidence (there is no distinction between ordinary and extraordinary beam for $\gamma_i = 0$). As can be seen, for high applied voltage (saturation condition $V_{\mathrm{rms}} = 48$ V) the transmittance is practically independent of the wavelength, but for a lower voltage (above-threshold condition $V_{\mathrm{rms}} = 24$ V) the PDLC is more transparent for red radiation than for blue-ultraviolet radiation. Even in saturation condition, at high values of the incidence angle (Fig. 9, sample transmittance versus the wavelength and the applied field for an extraordinary beam at incidence angle $\gamma_i = 60°$), the scattering coefficient for blue radiation is higher than that for red. Therefore the sample appears brown if illuminated with white light. Spectral distribution of the transmitted light is mainly controlled by the droplet radius, which in turn is determined by the curing procedure: however this is beyond the scope of this paper.

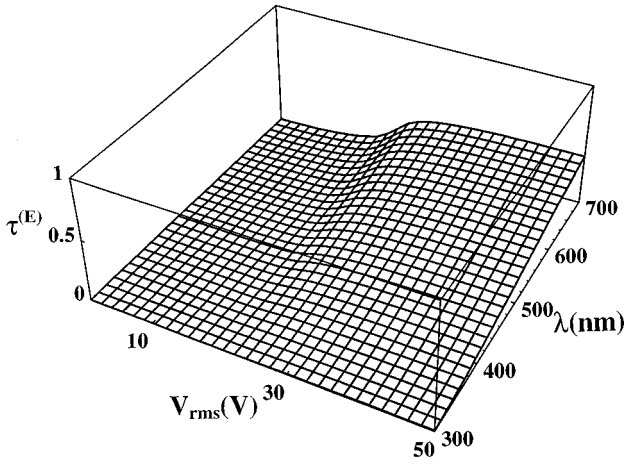

FIG. 9. Transmittance for an extraordinary beam vs wavelength and applied voltage, at incidence angle $\gamma_i = 60°$.

In conclusion, we have introduced a mathematical model capable of describing the transmittance of PDLC's in the most general conditions, which is not only for normally impinging light or high applied voltages but as a function of its geometrical and structural properties as well as of the operating conditions and of the incidence angle of impinging light. We have demonstrated the model accuracy by the comparison of numerical and experimental data. We have performed some parametric studies of PDLC optical behavior also in order to show the model effectiveness as a designing tool.

ACKNOWLEDGMENT

We acknowledge the technical aid of A. Maggio, S. Avallone, and S. Marrazzo.

[1] P. S. Drzaic, J. Appl. Phys. **60**, 2142 (1986).
[2] P. S. Drzaic, Liq. Cryst. **3**, 1543 (1988).
[3] B. G. Wu, J. L. West, and J. W. Doane, J. Appl. Phys. **62**, 3925 (1987).
[4] A. Fuh and O. Caporaletti, J. Appl. Phys. **66**, 5278 (1989).
[5] S. C. Jain and D. K. Rout, J. Appl. Phys. **70**, 6988 (1991).
[6] F. Bloisi, P. Terrecuso, L. Vicari, and F. Simoni, Mol. Cryst. Liq. Cryst. **266**, 229 (1995).
[7] J. W. Doane, N. A. Vaz, B. G. Wu, and S. Zumer, Appl. Phys. Lett. **48**, 269 (1986).
[8] P. G. de Gennes and J. Prost, *The Physics of Liquid Crystals* (Clarendon, Oxford, 1993).

[9] I. C. Khoo and F. Simoni, *Physics of Liquid Crystalline Materials* (Gordon & Breach, New York, 1992).
[10] W. H. de Jeu, *Physical Properties of Liquid Crystalline Materials* (Gordon & Breach, New York, 1979).
[11] M. J. Stephen and J. P. Straley, Rev. Mod. Phys. **46**, 617 (1974).
[12] S. Zumer and J. W. Doane, Phys. Rev. A **34**, 3373 (1986).
[13] S. Zumer, A. Golemme, and J. W. Doane, J. Opt. Soc. Am. A **6**, 403 (1989).
[14] F. Basile, F. Bloisi, L. Vicari, and F. Simoni, Phys. Rev. E **48**, 432 (1993).
[15] F. Basile, F. Bloisi, L. Vicari, and F. Simoni, Mol. Cryst. Liq. Cryst. **251**, 271 (1994).
[16] J. B. Whitehead, Jr., S. Zumer, and J. W. Doane, J. Appl. Phys. **73**, 1057 (1993).
[17] F. Bloisi, C. Ruocchio, P. Terrecuso, and L. Vicari, Opt. Lett. **21**, 95 (1996).
[18] J. R. Kelly and P. Palffy-Muhoray, Mol. Cryst. Liq. Cryst. **243**, 11 (1994).
[19] P. Palffy-Muhoray, M. A. Lee, and J. L. West, Mol. Cryst. Liq. Cryst. **179**, 445 (1990).
[20] S. Zumer, Phys. Rev. A **37**, 4006 (1988).
[21] M. Born and E. Wolf, *Principles of Optics*, 2nd ed. (Pergamon, New York, 1980).
[22] E. Dubois-Violette and O. Parodi, J. Phys. (Paris) Colloq. **30**, C4-57 (1969).
[23] F. Bloisi, C. Ruocchio, P. Terrecuso, and L. Vicari, Opt. Commun. **123**, 449 (1996).